6th European Conference For Aeronautics and Space Sciences, EUCASS, Krakov, Poland, June 29-July3 2015

EFFECT OF ATMOSPHERIC DRAG ON THE TRAJECTOIRIES OF SPACE DEBRIS AFTER A COLLISON

F. KEBE[1], Z. YIN[2], P. CLAUDE[2], M. DUDECK[2], D. HESTROFFER[1]

[1] Celestial Mechanics and Ephemeris Calculation Institute, IMCCE, Paris Observatory, CNRS, UPMC Pierre and Marie Curie University, Lille 1 University, France

[2] Institute Jean Le Rond d'Alembert, UPMC Pierre and Marie Curie University et CNRS, UMR 7190, 75005 Paris, France

Introduction

Space debris come from the upper stages of launch vehicles, representing the satellite's end of life and can also be a result of spacecrafts's or upper stages's explosions or collisions.
Today, the majority of catalogued space debris has been produced by accidental or intentional collisions between large spacecrafts.
In 2007, the weather satellite Fengyun 1C was intentionally destroyed by China by using a vehicle which rammed the satellite at a velocity close to 16 km/s [2]. The resultant collision created approximately 3,000 pieces of debris that continue nowadays to pose a threat to spacecrafts located in Low Earth Orbit (LEO). In 2009, the accidental collision between two communications satellites, the operational American Iridium-33 and the non operational Russian Cosmos 2251, greatly increased the number of large debris in currently orbit [1].
Collisions between space debris have also been reported in LEO [3].

Space debris are therefore mainly in LEO or in the geostationary orbit (GEO) and their number increases steadily (see Figures 1 and 2) increasing each year the risk of collisions, and posing a danger to satellites and space exploration missions.
The trajectories of the debris of size greater than 10cm are followed by observations from ground stations [4] which allows avoiding a collision with a satellite by moving it if it is equipped with a propulsion system which is the case for geostationary telecommunication satellites; these account for at least equal to 20 000 space debris according to the Space Surveillance Network - SSN, [5]. The millimeter sized space debris or smaller (dust clouds) do not represent a major risk to satellites. The intermediate sized debris are undetectable and present a risk of deterioration of a satellite in the case of a collision.

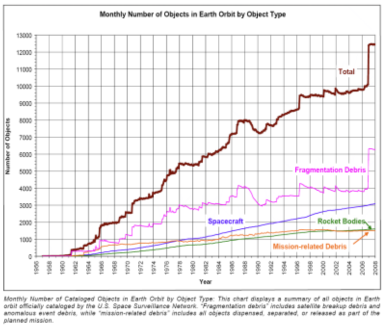

Fig. 1 Evolution of the number of debris (credit NASA)

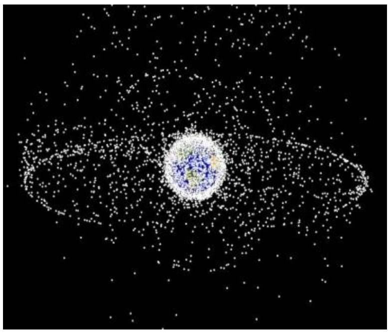

Fig. 2 Space debris in LEO and GEO (credit NASA)

Debris generated by a collision or by an explosion exists in a wide range of mass, energy (velocity increment) and directions.
A cloud of thousands of debris will therefore spread in space, and its coherent shape will disappear with time.

The nano-satellites are becoming more numerous in space, since the first launch of 6 Cubesats on 30th of June of 2003 from the Plesetsk Cosmodrome in Russia. Until 2012, a hundred Cubesats had been sent in space [6].
We present some properties of the cloud of 38,074 debris resulting from the collision between two Cubesats.
The distributions in mass and debris velocity increment is taken from NASA's fragmentation method [7].
The trajectory of such debris is calculated using the numerical of Runge-Kutta-Nystrom method.
The effect of drag on the ambient atmosphere is introduced using the exponential atmospheric model of Wertz [8], a drag coefficient and an equivalent cross section. The consideration of the perturbative effects of gravity related to the Sun and the Moon, the term J2 and solar radiation [9] is the following step of this study.

1. Space debris produced by the collision of two nano-satellites (Cubesats)

We study the debris produced by the collision of two Cubesats. The nanosatellite A, 1kg (Cubesat-1U), has a circular trajectory with a radius of 7,000 km. The trajectory of A is defined by $\Omega_A = 45$ ° and an inclination $i_A = 20$ °.
The nanosatellite B, 3kg (Cubesat-3U), has an elliptical trajectory with a semi-major axis a = 7,200 km, an eccentricity e = 0.2, $\Omega_B = 45$ ° and an inclination $i_B = 22$ ° (Fig. 3).

When the collision occurs at x = 3980 km, y = 5740 km, z = 433 km, the velocity of A is equal to 7.5461 km.s-1 (kinetic energy: 2.847 10^7 J) and the velocity of B is equal to 7,650 km.s^{-1}. (kinetic energy: 9.111 10^7 J).
At the moment of the impact the two velocity vectors form an angle of 1.389 rad.

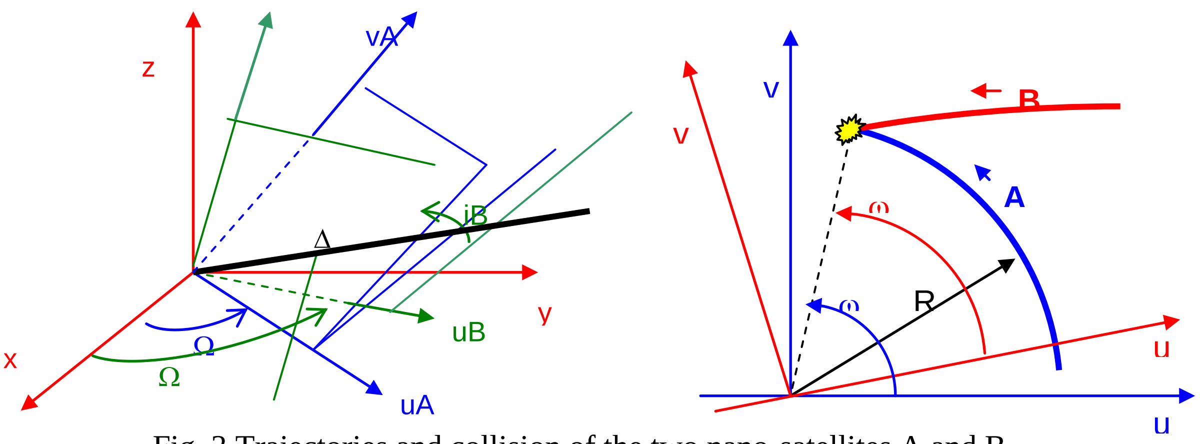

Fig. 3 Trajectories and collision of the two nano-satellites A and B

The number of fragments generated by the collision is given by the following formula taken from reference [7]:

$$N(L_c) = 0.1\ M^{0.75}.L_c^{-1.71}$$

with the mass M equal to the sum of the masses of the two objects involved in the collision (in kg) and the characteristic length Lc (in meters). Thus, for collision AB, M = 4 kg+3kg (A) and 1 kg (B). This relationship is based on terrestrial experiments of explosions and collisions.
The latest revision of the fragmentation model was made by NASA in 2001 [7].

The distributions in size and mass of debris are given by [7, 10, 11]. The determination of the mass m of a fragment is obtained by $m = \frac{1}{6}\pi d^3 \rho$. We consider that the fragments are spherical with a diameter d. In reality the assumption of sphericity greatly increases the error rate in determining the mass surface.
Thus, NASA replaced the diameter d by the characteristic size Lc, which allows us to consider that the fragments are not necessarily spherical.
This allows using the relationship giving “m” quoted above by replacing the diameter “d” by the characteristic size “Lc”.
The density ρ varies and depends on the size Lc by the following equation [7]:

$$\rho(L_c) = 92.937\ L_c^{-0.74}$$

with ρ in kg / m^3 and Lc in m.
This density decreases with the size of the debris and this also applies to fragments whose size is less than 1cm (density tends to infinity).
For the latter (Lc <1cm), it is considered that their density is constant and equal to the density of aluminum.
The number of fragments depending on the size and mass for collision between the two Nanosatellites A and B is given in Figure 4 and Table 1.

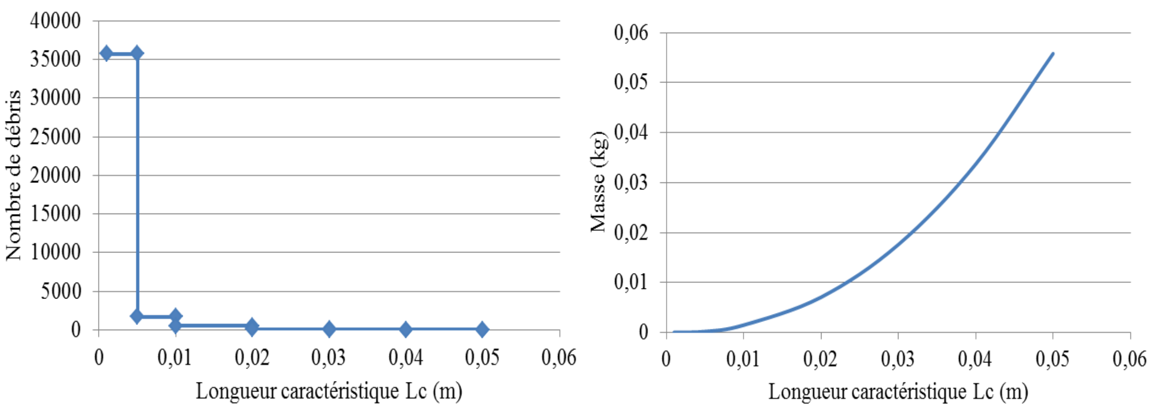

a) b)

Fig.4 Distributions of debris) in size, b) mass (mass of a debris of a population)

Characteristic length Lc (m)	Number of debris	Density of the debris (kg/m^3)	Mass of a debris (kg)
0.001	35720	2800	0.0000014661
0.005	1689	2800	0.00018326
0.01	516	2806.652	0.00146956
0.02	113	1680.453	0.00703907
0.03	44	1244.855	0.01759873
0.04	22	1006.153	0.03371653
0.05	10	853.003	0.05582895

Table 1. Distribution in size and mass of the debris generated by the collision of two nano-satellites A and B

These space debris are distributed into seven populations, ranging between 1 mm and 5 cm in size.

The largest debris has a mass equal to 55.83g.

The size of Cubesats and their masses restrict the number of generated debris. The largest size possible, due to the Cubesat-3U is equal to 30 cm, putting an upper limit to the characteristic length, Lc.

Once the number of debris is known, we can calculate their respective masses, beginning with the smallest debris.

We continue to calculate the mass until the total mass of the debris generated is equal to the mass of the two Cubesats (4 kg).

Thus, larger debris have a characteristic size that is equal to 5 cm. This value is consistent with the fact that the collision is considered “catastrophic”.

The number of debris decreases while their size increased, the number of debris is then equal to 38,114 and the total mass of the debris is 3.989 kg (≈ 3kg + 1kg). The ΔV increment velocity debris can be found from Su’s model [17]:

$$\begin{cases} \log\left(\frac{\Delta V}{V_M}\right) = A - B\left(\log\left(\frac{\Delta d}{d_M}\right)\right)^2, & if\ d \geq d_M \\ \log\left(\frac{\Delta V}{V_M}\right) = A, & si\ d < d_M \end{cases}$$

with

$$\begin{cases} A = 0{,}225 \\ B = 0{,}1022 \\ d_M = \dfrac{E_{c,M}^{1/3}}{6.194\ 10^7} \end{cases}$$

V_M and $E_{C,M}$ being respectively the velocity and kinetic energy of the largest object; the Cubesat 3U.

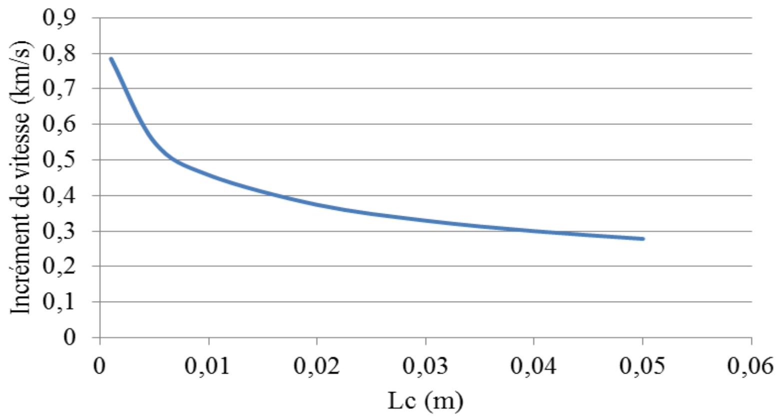

Figure 5. Velocity increments of debris depending on the characteristic length

The larger fragments are ejected with velocity increments much smaller than those of the small fragments. These increments vary from 0.27 m / s to 0.78 m / s for the collision A-B (Figure 5). The direction of the velocity increment of debris is taken randomly within a solid angle of 4π radians.

2. Space debris dynamics and atmospheric drag

The acceleration of a debris is given by:

$$m\vec{\gamma} = \vec{f}_{gravitationnelle} + \vec{f}_{frottement} + \vec{f}_{radiation} + \vec{f}_{Soleil-Lune}$$

where m is the mass of the debris and where $\vec{f}_{gravitationnelle}, \vec{f}_{frottement}, \vec{f}_{radiation}, \vec{f}_{Soleil-Lune}$ are the attraction of the Earth on the debris, the drag force on the ambient air, the force due to solar radiation, and the gravitational force due to the Sun and the Earth, respectively.

The Earth is assumed to be spherical, the gravitational force of the Earth $-m\frac{\mu_T}{r^3}\vec{r}$ where μ_T is the gravitational parameter of the Earth and r is the radius vector whose origin is the center of the Earth.

2.1 Drag on ambiant atmosphere

The drag force can be expressed in terms of a drag coefficient Cd, n, the density of the ambient air n and the velocity vector of debris $\vec{V}$ $\vec{f}_{frottement} = -\frac{1}{2}C_d\, A\, nV\vec{V}$. The drag force is in an opposite direction to the velocity vector $\vec{f}_{frottement} = -\frac{1}{2}C_d\, A\, nV\vec{V}$. It is therefore necessary to have an atmosphere model giving the density as a function of the altitude. The dynamics of a debris is therefore described through the acceleration

$\vec{a} = -\frac{\mu_T}{r^3}\vec{r} - \frac{1}{2}\frac{C_d\ A}{m} n(r) V \vec{V}$ where $\frac{C_d\ A}{m}$ is the balistic coefficient. A best description is obtained with the relative velocity $\vec{V}_{rel} = \vec{V} - \vec{V}_{atm}$ where $\vec{V}_{atm}$ is the local velocity of the ambient atmosphere, then $\vec{f}_{frottement} = -\frac{1}{2} C_d\ A\ n V_{rel} \vec{V}_{rel}$. No transverse acceleration is generally introduced. The drag is generally with a negative effect by the limitation of the lifetime of a satellite in LEO (the Cubesat Robusta has been de orbited only after 2years and half) but the effect is positive for the destruction of asteroid and debris.

2.2 Models of atmosphere

Numerous atmosphere models are available and the best choice of model is a compromise between the required precision of the trajectory and the computing time [15-2, 15-21]. The more popular models are the Patched Exponential Atmospheric model, the Mass Spectrometer and Incoherent Scatter Radar model MSISE-90, the CIRA model and the Jacchia atmospheric model. The last one is considered as the reference model.

. The model used is that of JR Wertz [8] which introduces 28 layers of which the last is at an higher altitude than 10000km.

In each layer, the density (kg.m^{-3}) is given by $\rho = \rho_0 e^{-\frac{z-z_0}{H}}$ where z is the geodetic height, H is a parameter which depends on the layer considered, ρ_0 is the density at z_0 (start of layer). This model does not account daily, seasonally and the point coordinates (latitude and longitude) and it can be used taking into account the flattening of the Earth.

The Jacchia model (1970) [Jacchia 14-2, 14-3,] introduces a calculation of the atmosphere densities between the altitude of 90 and 105 km with the barometric relation, and after 105 km with the diffusion equation. The Jacchia-70 model has been completed from the parameters which precise the spatial environmental situation such as solar declination and angular momentum, the exospheric temperature of the exosphere at the considered time is expressed with empirical expressions to deduce the densities of the various atmospheric species. The different steps of the calculation are described in [14-4]. The Jacchia model introduces detailed atmospheric conditions but its implementation in a numerical code is complex and increase the computing time.
The MSISE-90 model is similar to the Jacchia model. R. Whitmire [14-4] compared the atmospheric density variations as a function of the altitude for the three models (Jacchia-70, Exponential and MSISE-90). The exponential model exhibits the greater densities up to 1000km.

Other models can be used to express the drag force. A model commonly used takes into account the absorption of the air molecules and diffuse remission form in the case of a Maxwellian velocity distribution for a flat plate angled

relative to the speed, for a sphere and a cylinder in a free molecular regime for which volume collisions are negligible surface collisions[12,13].
The drag coefficient C_d is taken to be constant with a value between 1.8 and 2.2.

Air density can be also represented by the Jacchia model [15] for altitudes above 115 km and by the CIRA model to an altitude below 120 km.
The cross section A of the debris is normally counted in the velocity vector. It is estimated from the size of the debris by taking into account a correction factor.
The dynamics of the debris is thus described by the equation $\vec{\gamma} = -\frac{\mu_T}{r^3}\vec{r} - \frac{1}{2}\frac{C_d A}{m} n(r) V \vec{V}$.

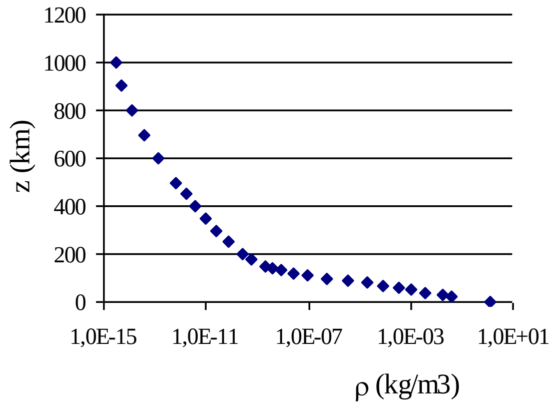

Fig.7 Density depending on the altitude from the atmospheric model of the Wertz exponential

2.3 Knudsen number and flow regime

The drag force depends on air flow conditions around the debris, the free molecular flow value when the Knudsen number is very large before generally considered Kn greater than 10, ($Kn = \frac{\lambda}{Lc}$ where Lambda is the mean free path of air particles and the characteristic dimension Lc of the debris). In this case the particles which collide with the debris have not collided before.

For a Knudsen number between 10^{-1} and 10, our goal is to model the transition the appearance of a thick shock and heat and kinetic slip parietal. For a Knudsen number less than 103 the system is continuous within a thin shock waves showing the absence of parietal slip.
Figure 6 shows the mean free paths in an atmosphere composed mostly of nitrogen and molecular oxygen in the same proportions as on the ground up to an altitude of 100 km and molecular nitrogen and atomic oxygen between 100 and 200 km.
This figure shows that the flow around a1mm molecular debris is free above about 85 km and above 100 km for a 5cm debris.

The mean free paths are deduced from the relation $\lambda = \dfrac{1}{\sqrt{2}\, n\sigma}$ where *n* is the density and σ is the cross section.

For an altitude up to 100km, we calculated the mean free paths from the relations,

$$\lambda_{N2-N2} = \frac{1}{\sqrt{2}\, n_{N2}\, \sigma_{N2-N2}}, \quad \lambda_{O2-O2} = \frac{1}{\sqrt{2}\, n_{O2}\, \sigma_{O2-O2}}, \lambda_{N2-O2} = \frac{1}{\sqrt{2}\, n\sigma_{N2-O2}}$$

where $n_{N2-N2} = X_{N2}.n$, $n_{O2-O2} = X_{O2}.n$ with the constant molar fractions $X_{N2}. = 0{,}79, X_{O2} = 0{,}21$ and with cross sections obtained by the hard sphere model ($D_{N2}. = 0{,}292..nm, 2R_{O2} = 0{,}315nm$).

For an altitude from 100km to 200 km, the mean free paths are,

$$\lambda_{N2-N2} = \frac{1}{\sqrt{2}\, n_{N2}\, \sigma_{N2-N2}}, \quad \lambda_{O-O} = \frac{1}{\sqrt{2}\, n_{O}\, \sigma_{O-O}}, \lambda_{N-O} = \frac{1}{\sqrt{2}\, n\sigma_{N2-O}}$$

where $n_{N2-N2} = X_{N2}.n$, $n_{O-O} = X_{O}.n$ with the constant molar fractions $X_{N2}. = 0{,}66 X_{O} = 0{,}33$ and with cross sections also obtained by the hard sphere model ($R_O = 60\, pm$).

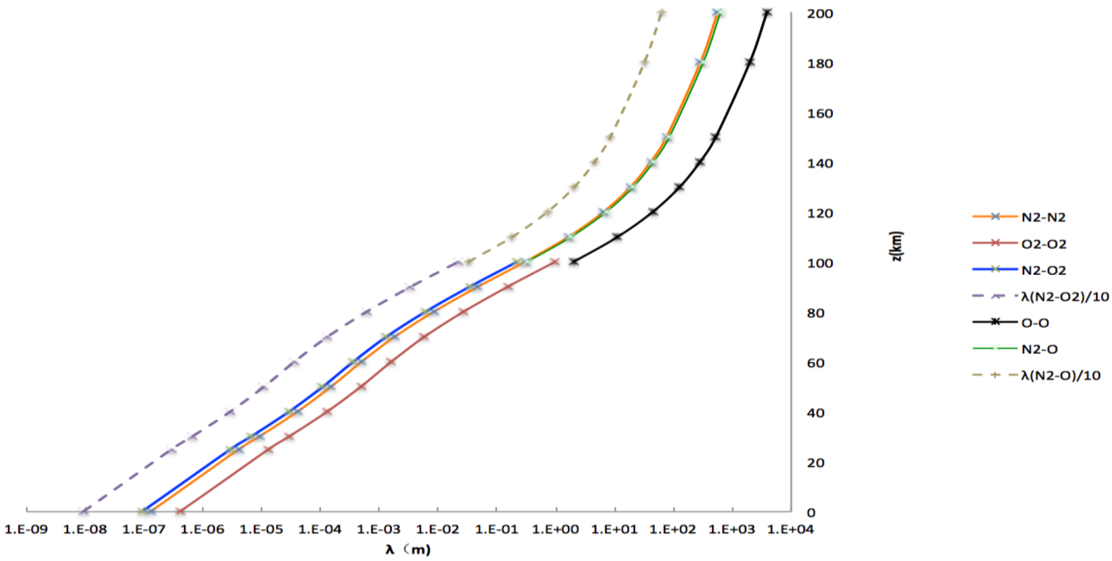

Fig.6 Calculated mean free paths as a function of altitude up to 200 km

2.4 Cross sectional aera

Furthermore, we consider the cross section A of the debris (normal to the path) without clear need to specify in detail the form and irrespective of any own rotational movement.

We assume that the expression of the cross sectional area A is:

$$A = \pi \frac{L_c^2}{4}$$

with eventually a correction factor.

2.5 Drag coefficient

A model commonly used to calculate the drag coefficient is to take into account the absorption of the air molecules and the remission under a diffuse form in the case of a Maxwellian velocity distribution for a flat plate angled relative to the speed for a sphere and a cylinder in a free molecular regime for which collisions in volume are negligible compared to the collisions in surface [12, 13].
G. Alphonso et al [14-5] expressed the drag coefficient as a function of the thermal velocity of the gas and VT of the object velocity V,
G. Alphonso et al [14-5] expressed the drag coefficient as a function of the thermal velocity V_T of the gas and of the object velocity V, $C_d = \delta[2 + \frac{4}{3}(\frac{V_T}{V})^2 - \frac{2}{15}(\frac{V_T}{V})^4]$ where δ is an accommodation coefficient (value between 1 and 2). G. Alphonso et al give values of the drag coefficient for hydrogen, helium and oxygen and for different gas temperatures. This coefficient can be estimated by H. Fraysse [15-3]).et al if a simple geometric configuration is assumed (sphere, cylinders, cones) without rotation. The drag coefficient for a plate is expressed with two contributions, the first one C_d^a is due to surface absorption of the particles and the second one C_d^r is due to the re-emission effect. These two coefficients are function of the gas and surface temperatures, of the relative velocity, of the mean molar gas and of incidence angle relative to the surface. From these expressions, a mean value of the drag coefficient vs altitude is deduced and increasing from 2.08 at 125 km to 2,96 at 1350 km. V.L Pisacane [15.6] suggests a drag coefficient of 2.2 for plate elements and about 2.0 or 2.1 for spheres. In [15-7] it's indicated that for 7 satellites with a mass from 5 kg to 76,136 kg, the drag coefficient is always lower than 4.
The dimensionless drag coefficient C_d will be taken constant during the reentry with a value between 1,8 et 2,4. The typical value of 2.2 will be retained in our calculations.

3. Numerical method

Many methods have been proposed to calculate the trajectory of an object in space.

The method used to calculate the trajectory of the debris is that of Runge-Kutta-Nystrom [15] and uses the following relations.

$$
\begin{cases}
k_1 = \frac{h^2}{2} f(x_r, y_r, y_r') \\
k_2 = \frac{h^2}{2} f\left(x_{r+\frac{1}{2}}, y_r + \frac{h}{2} y_r' + \frac{1}{4} k_1, y_r' + \frac{1}{h} k_1\right) \\
k_3 = \frac{h^2}{2} f\left(x_{r+\frac{1}{2}}, y_r + \frac{h}{2} y_r' + \frac{1}{4} k_1, y_r' + \frac{1}{h} k_2\right) \\
k_4 = \frac{h^2}{2} f\left(x_{r+1}, y_r + h y_r' + k_3, y_r' + \frac{2}{h} k_3\right) \\
y_{r+1} = y_r + h y_r' + \frac{1}{3}(k_1 + k_2 + k_3) \\
y_{r+1}' = y_r' + \frac{1}{3h}(k_1 + 2k_2 + 2k_3 + k_4)
\end{cases}
$$

For each integration time step this method calculates the value of the intensity of gravity.

This method was tested first in several cases of circular (r = 6778.14 km) and elliptical (e = 0.7, a = 22630.363 km) trajectories over a period T and over a period of 30 years.

To ensure the accuracy of the program, we made the calculation without perturbations effect with several time (from 0.01s to 2s) calculating the error Δr on the altitude and the error Δd on the distance from the starting point over a period n.T.
For example, for a circular orbit with a time step of 0.4s, after one year (t = nT~ 1 an) $\Delta r = 2.3\ 10^{-9}$ m, $\Delta d = 4.71\ 10^{-5}$ m and after 100 years (t = nT~ 100 ans), $\Delta r = 1.55\ 10^{-7}$m, $\Delta d = 0.131$ m.

For the elliptical orbit with a step time 0.09s, after one year (t = nT~ 1 an) , $\Delta r = 1.82\ 10^{-09}$m, $\Delta d = 1.21\ 10^{-04}$ m and after 100 years (t = nT~ 100 ans) , $\Delta r = -1.23\ 10^{-7}$ m, $\Delta d = 6.49\ 10^{-2}$ m.

The RKN algorithm gives results whose accuracy is satisfactory for our cloud study. We will gradually add the disruptive forces starting with the drag force on the air.

4. Results

Figure 8 shows the evolution of the apogee and perigee for some debris produced by the collision of two nano-satellites A and B taking into account the drag on the atmospheric layers (atmospheric model Wertz, C_d drag coefficient constant).

From the state vectors of the two Cubesats, we calculated the state vector of the collision. Thus, it occurs at the point (x = 3980.8 km, y = 5740 km, z = 433.641 km) at a speed whose components are those of the average speed of A and B are: Vx = -5.272 km/s, Vy = 2.728 km/s, Vz = 2.271 km/s.

At these initial conditions, we add to the speed increment of components speed of the collision. We will study the trajectory and the orbital elements of the following debris chosen as examples:

Number of the debris	Characteristic length Lc (m)	Mass (kg)	Section A (m^2)	Speed Increment

				(km/s)
1	0.001	1.466E-06	7.85E-07	0.784
2	0.005	1.83E-04	1.96E-05	0.549
3	0.01	1.47E-03	7.85E-05	0.457
4	0.02	7.04E-03	3.14E-04	0.373
5	0.03	1.76E-02	7.06E-04	0.329
6	0.04	3.37E-02	1.25E-03	0.299
7	0.05	5.58E-02	1.96E-03	0.277

Table 2. Input data of the four studied debris

The debris speed increments were decomposed randomly via a function available in Matlab.

Number of the debris	Lc (m)	Increment speed (km/s)	ΔVx (km/s)	ΔVy (km/s)	ΔVz (km/s)
1	0.001	0.784	0.766	-0.08	-0.145
2	0.005	0.549	0.441	0.0124	0.327
3	0.01	0.457	-0.035	-0.452	0.06
4	0.02	0.3737	0.18	-0.109	-0.308
5	0.03	0.329	-0.161	0.279	0.065
6	0.04	0.299	-0.207	-0.179	-0.12
7	0.05	0.277	0.084	-0.062	0.257

Table 3. Values of speed increments components

The trajectory of the debris will be studied in 3 cases:

- Under the influence of the atmospheric drag
- Under the influence of the atmospheric drag and the Earth's rotation
- Under the influence of the atmospheric drag, the Earth's rotation and the influence of J2 perturbation

We consider that the debris entered the atmosphere when its altitude is equal to 120 km.

Case A:

Here, the reentry of the seven debris are calculated by considering solely the effect of atmospheric drag.

Debris number	Time of reentry (min)
1	7min39s
2	8min11s
3	5min40s
4	6min47s

5	8min43s
6	6min16s
7	7min20s

Table 4. Reentry of the 7 debris

The debris fall into Earth at different times:

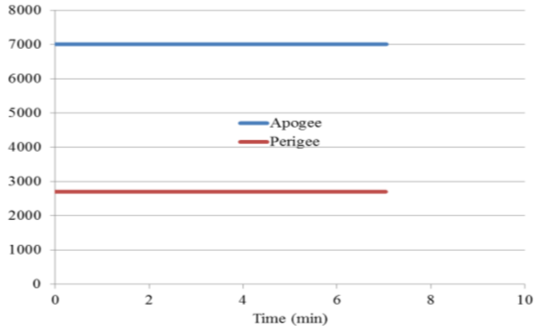

Debris 1

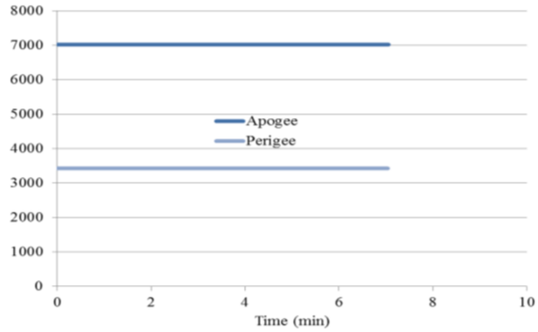

Debris 2

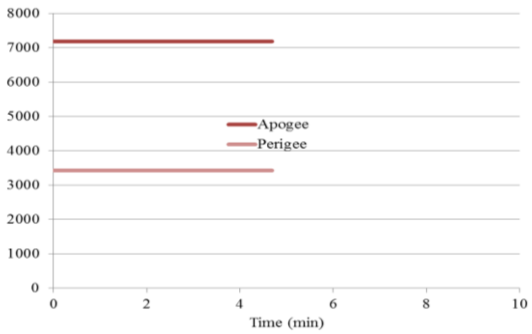

Debris 3

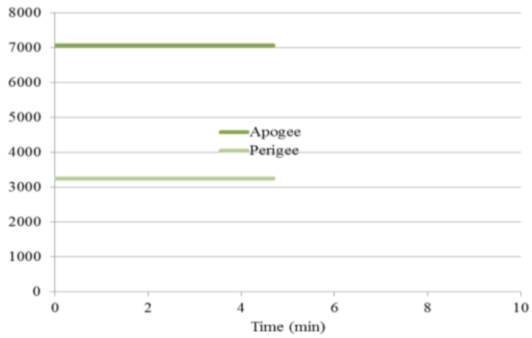

Debris 4

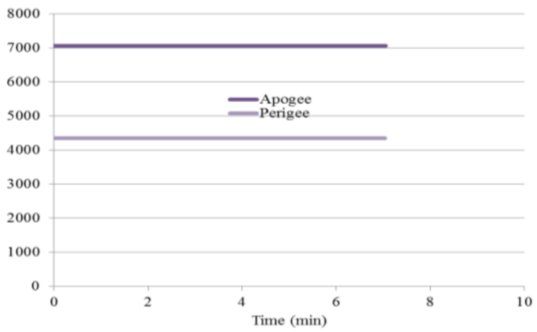

Debris 5

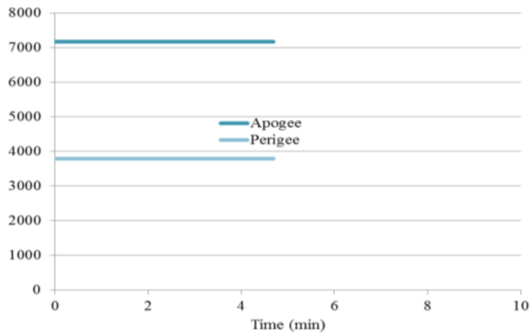

Debris 6

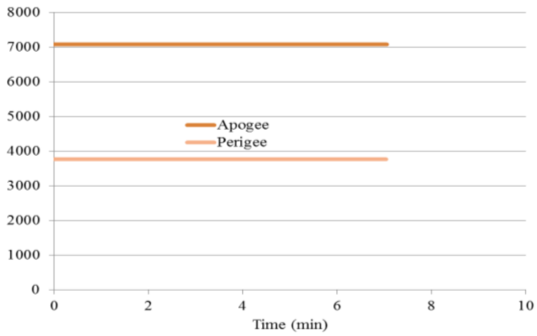

Debris 7

Fig 8. The apogee and perigee of the debris

Case B and case C:

The results of the cases B and C show similar results as the case A. Thus, the influence of the term J2 and the Earth rotation on the debris is very small. Concerning the term J2, its negligible influence is due to the short lifetime of the debris.

Conclusion

The purpose of this work is to investigate the issues posed by the exploitation of Cubesats in Low Earth Orbit. The goal is to develop a tool that will help in the regulation and legislation for Cubesats.

The effects the atmospheric drag, the Earth's rotation and the influence of J2 perturbation on cm-sized debris have been quantified in Low Earth Orbit. Thus, those particles don't stay for a significant time in space.

In case of an explosion or collision between Cubesats, depending on their position, most of the generated space debris will have a short lifetime. In view of this, the Cubesats should be located at a precise region as a prevention process.

The developed code will be more precise by introducing the gravitational effect of the Moon and the Sun and the radiation pressure effect of the Sun. These introductions need to know the date of re-entry and will be done after the tests on different atmosphere model. Finally, the whole debris cloud will be studied.

References

[1] J.-C. Liou, , N.L. Johnson, Characterization of the cataloged Fengyun-1C fragments and their long-term effect on the LEO environment, Advances in Space Research, Volume 43, Issue 9, Pages 1407–1415, 1 May 2009

[2] Ch. Lardier, Destruction orbitale involontaire, Air et Cosmos n°2160, 20 février 2009

[3] D. J. Kessler, et al., Orbital Debris Environment for Spacecraft Designed to Operate in Low Earth Orbit, NASA TM 100 471, Johnson Space Center, Houston, TX, 1989

[4] S.-Y. Su, D.J. Kessler, Contribution of explosion and future collision fragments to the orbital debris environment, Advances in Space Research, Volume 5, Issue 2, 1985, Pages 25–34

[5] United States Air Force Scientific Advisory Board, Report on Space Surveillance, Asteroids and Comets, and Space Debris, SAB-TR-96-04, Volume I: Space Surveillance June 1997

[6] M. Swartwout, The First One Hundred CubeSats: A Statistical Look: JoSS, Vol. 2, No. 2, Pages 213-233, 2013

[7] N.L. Johnson, P.H. Krisko, J.C. Liou and P.D. Anz-Meador, NASA's New Breakup Model of EVOLVE 4.0, Advances in Space Research, Vol. 28, N° 9, Pages 1377-1384, 2001

[8] D.A. Vallado, Wayne D. McClain, Fundamentals of Astrodynamics and Applications Springer Science & Business Media, 958 pages, 30 juin 2001

[9] A.E. Roy, Orbital Motion, Fourth Edition, CRC Press, 544 Pages, 31 déc. 2004

[10] M. Rossi, Upgrade of the Semi-Deterministic Model to study the long term evolution of the space debris", Final report, ESA/ESOC Contract No. 15857/01/D/HK(SC)

[11] R. C. Reynolds, Review of current activities to model and measure the orbital debris environment in low Earth orbit, Advances in Space Research, Volume 10, Issues 3–4, Pages 359–371, 1990

[12] A. Rossi, A. Cordelli, C. Pardini, L. Anselmo, P. Farinella, Modelling the space debris evolution: two new computer codes, Advances in the Astronautical Sciences, Spaceflight Mechanics, 1995
[13] S.-Y. Su, The velocity distribution of collisional fragments and its effect on future space debris environment, Advances in Space Research, Vol. 10, No. 3-4, Pages 389-392, 1990
[14] H. Fraysse, V. Morand, C. Le Févre, F. Deleflie, S. Waillez, A. Lamy, Th. Martin, E. Perrot, Long term orbit propagation techniques developed in the frame of the French space act, 5th IPASS Conference: A Safer Space for a Safer World, Versailles, France, 17-19 Oct. 2011
[14] R. Biancale, Les forces perturbatrices, Ecole de Géodésie Spatiale, Forcalquier, France, 2-6 Septembre 2002
[15] L. Collatz, The Numerical Treatment of Differential Equations, Third Edition
[16] LAW n° 2008-518 of the 3rd of June 2008 on Space Operations
[17] D.S. Mc Knight, Determination of breakup initial conditions, J. Spacecraft, Vol. 28, N° 4